Proceedings of the 8th International Symposium on Cavitation
CAV2012 - Abstract No. 210
August 14-16, 2012, Singapore

SPATIAL AND TEMPORAL HIGH RESOLUTION MEASUREMENT OF BUBBLE IMPACTS

Sebastian Lang
Chair of Fluid Systems Technologies
Technische Universität Darmstadt
Germany

Martin Dimitrov
Chair of Fluid Systems Technologies
Technische Universität Darmstadt
Germany

Peter F. Pelz
Chair of Fluid Systems Technologies
Technische Universität Darmstadt
Germany

SUMMARY

The present paper deals with a feasibility study of a new cavitation measurement method developed at the *Chair of Fluid Systems Technologies* (TU Darmstadt). The measurement principle is based on the piezoelectric attributes of a thin PVDF-membrane. The eigenfrequency of the membrane in the range of GHz in combination with a special sampling concept by means of an electrode matrix enable the measurement principle to measure pressures both temporally and spatially resolved.

Pressure histories generated by cloud cavitation are investigated by means of the new measurement method and comparisons with high-speed photographs give very promising results concerning the qualitative statements delivered with the measurement signals of the sensor. Furthermore, statistical evaluations of the intensity of the measured pressure signals were carried out and are in good agreement with results from damage experiments.

INTRODUCTION

Scientists and engineers need to measure cavitation for several reasons: On the one hand it is necessary to identify the occurrence of cavitation during development in order to define critical operating conditions for components of fluid systems. On the other hand, e.g. if there is no possibility to avoid these critical operating conditions over the whole lifetime of a component, it is important to know where and how much erosion due to cavitation has to be expected for a given operating condition. As the damage causing cavitation bubble impacts happen very fast and spatially distributed, their temporal and spatial resolved measurement is one of the most difficult challenges in cavitation research.

Today, the identification of critical operating conditions is often done with the help of pressure transducers. They are usually applied inside the channel walls and record a temporally resolved but spatially averaged signal of the pressure inside the liquid. Transfer functions influence these high frequency pressure signals on their way from the locations of bubble impacts to the sensor which makes a correct interpretation of the signals very difficult. In contrast to that, the prediction of the locations of highest cavitation damage is usually performed with erosion experiments. In these experiments, soft metal layers are used as "material sensors" and investigated after the damage experiments by means of optical measurement systems. The well-known Pit-Count method, developed during the last decade in Grenoble (France) and Darmstadt (Germany), is an example of such cumulative measurement methods (see e.g. [1]). These methods provide spatially resolved but temporally cumulated impressions of the damages caused by cavitation. A major problem of this kind of investigations is the time effort single measurements take.

In this paper, a new cavitation measurement method developed at the *Chair of Fluid Systems Technologies* (TU Darmstadt) will be presented. It is based on a piezoelectric membrane which serves as pressure transducer and an electrode matrix that enables the electrical measurement system to record spatially distributed voltage signals over the membrane. With this measurement principle, pressure signals can be recorded both temporally and spatially resolved and thus the advantages of the two classical measurement methods mentioned above are combined. The piezoelectric membrane itself has already been successfully applied e.g. by [2] as a pulse detector for triggering of a high-speed camera.

To validate our new measurement method, tests were carried out in a test bench that is designed in such a way that cloud cavitation arises inside the divergent part of a convergent-divergent nozzle. The pressure histories recorded with the new sensor are first compared qualitatively with photographs taken by a high-speed camera. After that, the measured signals will be investigated by means of statistical data analysis and compared with experimentally determined damage maps to evaluate the sensor's ability to predict the locations of highest cavitation erosion.

MEASUREMENT METHOD

The new sensor employs the piezoelectric effect of a thin PVDF (polyvinilidenfluorid, $C_2H_2F_2$) membrane. When mechanical normal stress (e.g. liquid pressure Δp) deforms the membrane in the direction of thickness, the electric charges inside the material are displaced and a difference in electrical potential be-

tween the upper and lower side of the membrane arises. The electric voltage ΔU between these two potentials serves as a direct measure for the pressure difference

$$\Delta p = \frac{\varepsilon}{b\, d_{33}} \Delta U \tag{1}$$

that was applied to the membrane. In Eq. (1) ε is the material's permeability, d_{33} is the material's piezoelectric distortion coefficient and b is the thickness of the membrane.

Due to a comparable high Young's modulus of the material (range of $10^9\,\mathrm{N/m^2}$), the first eigenfrequency of the membrane is in the range of GHz and thus much higher than that of conventional pressure transducers. This means that the measured pressure signals are allowed to be much more dynamical than in case of conventional pressure measurement methods. Hence our measurement principle is most suitable to deliver the temporal resolution needed to identify cavitation impacts.

A special electrical design is employed in order to realize the spatial resolution of the sensor. The spatial resolved recording of voltage signals is based on a matrix formed by electrode rows on the upper and lower side of the membrane which are oriented in an orthogonal way to each other (Fig. 1).

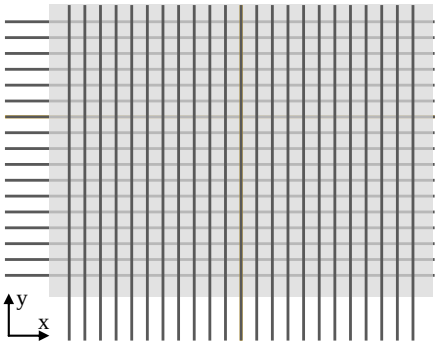

Fig. 1: Principle of electrode rows and columns.

By measuring the differences in electrical potential between one electrode oriented in x-direction against all electrodes oriented in y-direction, e.g. a spatially resolved measurement of voltage distributed on a line oriented in x-direction can be carried out. The principle described above can easily be extended to a spatially resolved measurement of a whole area, of course. Every combination of one electrode oriented in x-direction and one electrode oriented in y-direction represents a single pixel of the sensor.

The spatial resolution achieved with a former sensor prototype manufactured at the *Chair of Fluid Systems Technologies* was $12\,\mathrm{pixels/mm^2}$. This pixel density is the current state of the art in manufacturing of flexible circuit boards. In contrast to that, the achieved temporal resolution very much depends on the measurement electronics used for recording the voltage signals. In case of conventional measurement electronics like multi-channel data acquisition boards, the sampling rate also decreases with increased number of recorded pixels.

The prototype of our sensor presented in this paper has a pixel size of 2 mm x 2 mm with a a pixel distribution of 32 x 32. Due to a lack of measurement electronics fast enough to record all 1024 pixels of our sensor with sufficient sampling rate, we restrict ourselves to the spatial resolved measurement of a line of 32 pixels in this paper. The data acquisition is done with a 32-channel measurement card with a maximum total sampling rate of 1 GHz. This card is able to acquire the voltage signals of all 32 pixels of the line with a sampling rate of 31.25 kHz which is sufficient to detect the macroscopic pressure histories generated by cloud cavitation. Macroscopic in this case means that the pressure histories of the cloud collapses can be resolved for qualitative analysis. In contrast to that, the pressure histories of all single bubbles collapsing during the cavitation cloud collapses can not be resolved with the current sampling rate and spatial resolution.

To further increase the number of recorded pixels and the temporal resolution per pixel, faster recording electronics have to be developed in the proceeding of the sensor's development. At the moment we work on increasing the number of recorded pixels and want to achieve the range of 512 pixels with a sampling rate per pixel in the range of 20 MHz in the near future.

EXPERIMENTAL SETUP

The experimental validation of our new sensor was carried out in a test bench designed in such a way that cavitation arises in the divergent part of a convergent-divergent nozzle. Numerous investigations of the cavitation phenomena inside this nozzle have been carried out in e.g. [1] and [3] concerning the dynamics of the appearing cloud cavitation and the erosion caused by the collapsing cavitation clouds.

The geometry of the convergent-divergent nozzle is illustrated in Fig. 2. The channel has a rectangular cross section with walls completely made of acrylic glass in order to enable an excellent optical accessibility to the cavitation phenomena. The kinematics of the cloud cavitation are observed by means of high-speed photographs (frame rate 10 kHz) taken from a top view of the nozzle.

A small obstacle with rectangular cross section is applied to the narrowest position of the nozzle over the whole channel width. It has been investigated by [1] that this obstacle dramatically improves the homogeneity of cavitation in the narrowest cross section of the nozzle as side wall effects due to surface roughness are negligible in comparison to the influence of the obstacle.

The type of cavitation arising in the nozzle depends on the operating condition indicated by the two dimensionless products cavitation number

$$\sigma = \frac{p_o - p_v}{\frac{\rho}{2}\bar{c}^2} \tag{2}$$

and Reynolds number

$$Re = \frac{\bar{c} H}{\nu}. \tag{3}$$

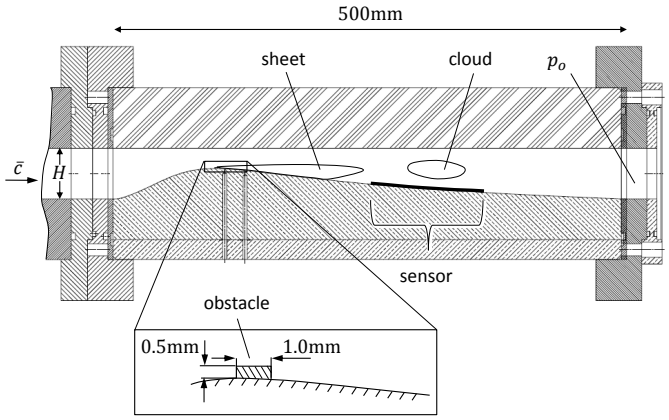

Fig. 2: Geometry of the convergent-divergent nozzle.

In Eq. 2 and 3 p_o denotes the static pressure at the nozzle outlet, $\bar{c}$ is the mean flow velocity and H is the channel height far away from the nozzle inlet, p_v denotes the vapour pressure, ρ the density and ν the kinematic viscosity of the liquid.

The cavitation phenomena observed in the nozzle vary between sheet and cloud cavitation depending on the operating condition of the nozzle. For a given cavitation number the flow will stay in the mode of sheet cavitation up to a critical Reynolds number. Beyond this critical Reynolds number, the observed cavitation phenomenon changes to a more aggressive form called *periodic cloud cavitation*.

In these operating conditions above the critical Reynolds number, a cavitation sheet grows with its front edge fixed to the obstacle in the narrowest cross section of the nozzle (see Fig. 2). When a maximum sheet length is reached, a so called re-entrant jet infiltrates the sheet upstream and finally leads to a complete detachment of the sheet's front edge from the obstacle. The sheet respectively cloud is then washed downstream by the liquid flow and collapses when a region of static pressure with sufficient magnitude is reached. Already during this violent collapse of the cavitation cloud, a new cavitation sheet begins to grow with its front edge fixed to the obstacle and the next cloud cavitation cycle starts. For a more detailed discussion on the dynamics of cloud cavitation see e.g. [1] or [4].

Keil & Pelz [1] further investigated the aggressiveness of cloud cavitation as a function of the operating point. They analysed numerous operating conditions with varying cavitation number and Reynolds number by means of damage experiments (Pit-Count) and found out that the amount of surface damage increases on the one hand with decreasing cavitation number and on the other hand with increasing Reynolds number.

To measure the pressure impacts generated by collapsing cavitation clouds, our sensor foil is applied to the curved nozzle surface by means of acrylate adhesive with a thickness of roughly $8\,\mu$m. As the cloud collapses happen some way downstream of the narrowest position of the nozzle, the sensor was positioned in such a way that its most upstream edge is located 100 mm downstream of the obstacle (see Fig 2). The sensor has a quadratic shape with an edge length of approximately 64 mm.

We restrict the investigations with our sensor to only one operating point characterized by $\sigma = 5.45$ and $Re = 2.75 \text{ x } 10^5$ in this paper. This point was chosen to have a good compromise between well measurable and not too damaging cloud collapses in order to maintain the intactness of our sensor prototype during the whole measurements.

RESULTS

The voltage signals acquired from the sensor are massively disturbed by the asynchronous motor driving the pump for the test bench. In fact, the sensor prototype is very sensitive to electromagnetic disturbances as its impedance is comparatively high. Since the disturbances caused by the asynchronous motor occur with grid frequency 50 Hz respectively with its third harmonic at 150 Hz, they can easily be filtered from the signal. This filtering is done with help of 4th-order IIR band-stop filters with bandwidths of 3 Hz and center frequencies of 50 Hz respectively 150 Hz for all measured values presented in this paper. The effect of these filters is concentrated mainly at the two frequencies named above, as can be seen in the exemplary amplitude spectra of a raw signal acquired from one pixel and its corresponding filtered signal shown in Fig. 3. Since the filtering is applied to all measured channels, no further considerations about phase shifts caused by the filtering have to be carried out.

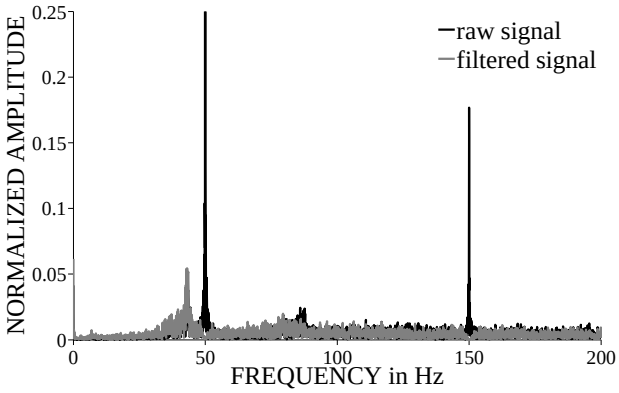

Fig. 3: Exemplary frequency spectra of raw and filtered measurement signal of one pixle.

The peak amplitude of the filtered signal lies at approximately 43 Hz (see Fig. 3) which is in very good agreement with the cloud collapse frequency determined from the high-speed photographs.

To show the sensor's ability of measuring pressure both temporally and spatially resolved, the history of measurement signals distributed on a line of 32 pixels in flow direction was measured during one cloud collapse and will be analysed qualitatively in the following. Different moments of the collapse are illustrated with high-speed photographs in Fig. 4. The locations of the 32 pixels are indicated with a black line. The length of that line equals 64 mm. The flow direction in the photographs is from left to right.

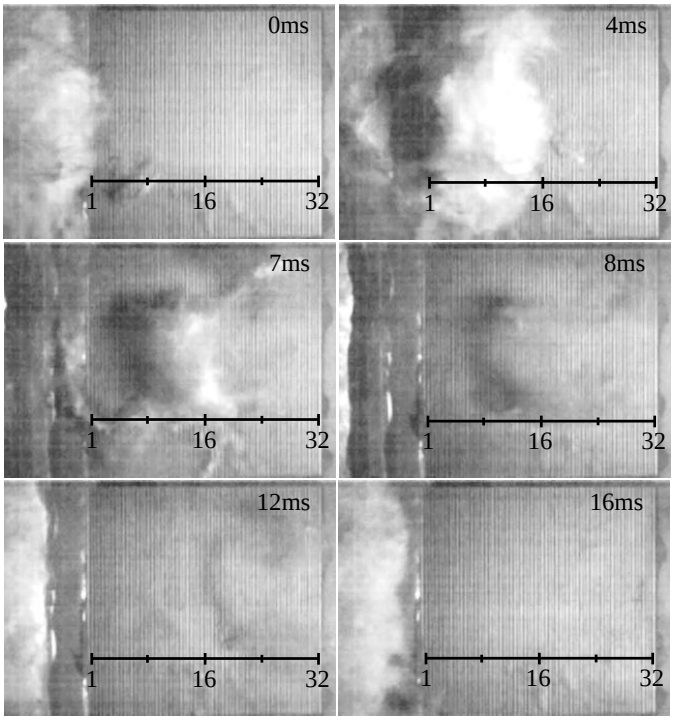

Fig. 4: High-speed photographs taken at different moments of one cloud collapse (black line indicates location of measured pixel line, flow direction is from left to right).

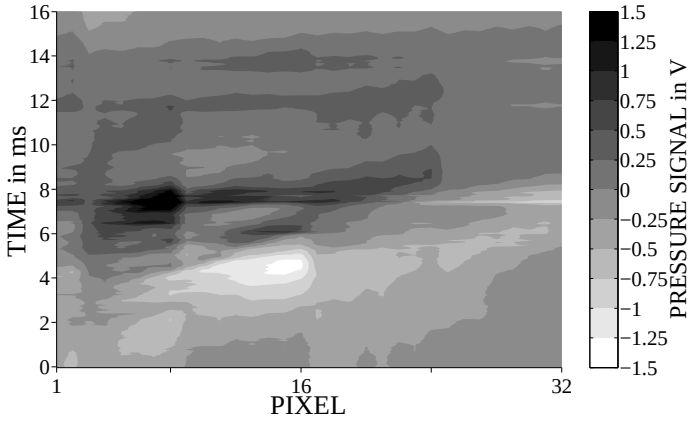

Fig. 5: Pressure signal history of all 32 pixels during one cloud cycle corresponding to the high-speed photographs shown in Fig. 4.

Fig. 5 shows the measurement signals of all 32 pixels over time in form of a contour plot. Darker contours indicate higher measured voltages and thus positive pressure changes on the surface of the sensor. As the PVDF-membrane works capacitive, negative voltages appear when a negative pressure change leads to an absolute pressure smaller than a reference pressure which would cause an undeformed membrane. Due to random charge or discharge of the PVDF-membrane (e.g. by electromagnetic radiation or the sampling of the measurement card) the value of this reference pressure is not ascertainable from the sensor signals and hence no absolute pressures can be measured with the sensor.

The sensor was calibrated by means of predefined pressure changes at the *Chair of Fluid Systems Technologies*. The sensor constant was determined as $\varepsilon / b\, d_{33} \approx 1575\,\mathrm{kPa/V}$ and will be applied for conversion from positive changes of the measured voltages to pressure changes in the following. As the reference pressure described above is time-dependent and not known, Fig. 5 only shows the measured voltages instead of pressures calculated by means of Eq. 1.

Nevertheless, the qualitative results shown in Fig. 5 together with the calculated pressure changes given in the text offer a good impression of the sensor's capabilities.

At the beginning of the collapse cycle (see Fig. 4 at 0 ms), the cloud is in front of the sensor and the measured signal of all 32 pixels lies slightly below 0 V. During the time until 4 ms, the cloud moves above the sensor and the pressure signals of all pixels decrease: The pixels located more upstream show the decrease earlier than those located more downstream. A minimum pressure signal is observed at approximately 4 ms above pixels 10 to 15 which are located directly below the cavitation cloud at this moment.

During the time from 4 to 7 ms, the size of the cavitation cloud decreases beginning from the part of the cloud located most upstream. Thus a temporally distributed increase of the pressure signal on the pixel line can be observed during that time: The pixels located more upstream show the increase earlier than those located more downstream.

The collapse of the rest of the cavitation cloud happens in a short time period of approximately 0.3 ms between 7 ms and 8 ms (see Fig. 4). During that time, peaks in the pressure signals of pixels 1 to 16 can be observed without visible time delay. This is in very good agreement with the position of the cloud just before the collapse: Only the top of the cloud can be seen in the photographs of Fig. 4. The base of the cloud is usually located some way more upstream than its top, because the local flow velocities near the nozzle surface are smaller than those at intermediate channel heights (see [1] or [4] for a more detailed discussion on cloud kinematics). The maximum positive pressure change calculated with help of the calibration factor and Eq. 1 from the positive change of the measured voltage of pixel 8 between 4.1 ms and 7.4 ms is approximately 4.3 MPa (2.75 V).

A second pressure peak with much smaller amplitude can be observed at 12 ms above pixels 4 to 23. This peak is caused by a rebound of the cavitation cloud that is hardly recognizable in the high-speed photographs. Only the shadow above pixels 7 to 14 in the photograph corresponding to time 8 ms and its disappearance until 12 ms indicate that some vapour regions remained after the main collapse at 7.4 ms.

During the time from 12 to 16 ms all vapour above the sensor is washed away or condensed and the sensor signals return to values slightly below 0 V for all pixels as in the beginning of the collapse cycle.

DISCUSSION

The maximum pressure amplitude measured with the sensor was 4.3 MPa. This value is in very good agreement with pressure amplitudes measured by other authors by means of conventional pressure transducers: [5] for example measured maximum amplitudes of 4 MPa for the case of cloud cavitation at an oscillating hydrofoil.

Nevertheless, these amplitudes are much smaller than the typical yield strength of copper (range of 200 MPA) which was used by [1] as "material sensor" to generate damage maps with help of the Pit-Count method. This means that the temporal and spatial resolutions of our measurement method are still not sufficient in order to resolve the damage causing events that happen among the macroscopic cloud collapses.

The peaks of the measurement signal in Fig. 5 caused by the cloud collapse (8 ms) and the rebound (12 ms) seem to appear at all pixels surrounding the collapses at the same time. In contrast to that, the beginning of the cloud collapse is expected to be a spatially distributed phenomenon and thus some kind of pressure wave should be observed in the measurement signals of different pixels. As this is not the case, the sampling rate chosen for the measurements seems to be too small for the resolution of pressure waves in the liquid.

To show our sensor's capabilities in prediction of the areas of highest expected cavitation damage, a qualitative comparison between statistically evaluated measurement signals from the sensor and an experimentally determined damage map from [1] is carried out in the following. Both measurement methods were applied to the operating point characterized by $\sigma = 5.45$ and $Re = 2.75 \text{ x } 10^5$ in the same convergent-divergent nozzle at the *Chair of Fluid Systems Technologies*. Nevertheless, slightly different cloud cycle frequencies were observed during the two experiments: [1] measured cloud detachment frequencies in the range of 38 Hz whereas we measured collapse frequencies in the range of 43 Hz for the given operating point (see chapter RESULTS). This difference is most likely caused by the small changes in geometry due to the application of our sensor instead of the copper foil which was used as material sensor by [1].

The quadratic amplitude sum

$$QAS = \sum_i \Delta\hat{p}_i^2 \, h_i \tag{4}$$

is used in order to quantify the damage potential of the pressure changes measured by each of the 32 pixels of a line of the sensor. In Eq. 4, $\Delta\hat{p}_i$ denotes the amplitude of a pressure change class appearing with probability h_i per time unit. The quadratic amplitude sum *QAS* is proportional to the energy of all pressure pulses per time unit and thus represents a measure for the intensity of a pressure signal (see e.g. [6]). As the quadratic amplitude sum defined in Eq. 4 uses pressure changes, the calibration factor introduced in chapter RESULTS can be applied and the quadratic amplitude sum will be given in MPa^2/s in the following. The evaluation of our sensor's measurement signals by means of *QAS* is limited to 4.5 s of the cloud-cavitating flow. This measurement time equals approximately 190 cloud cycles for the given operating point.

Fig. 6 shows the damage map for the given operating point determined by [1] by means of the Pit-Count method in the upper half and the quadratic amplitude sum *QAS* plotted over the line of 32 pixels in the lower half. The absolute position of the pixel line inside the nozzle and especially in relation to the damage map is indicated by the black line drawn over the damage map in the upper half of Fig. 6. The flow direction in Fig. 6 is from left to right.

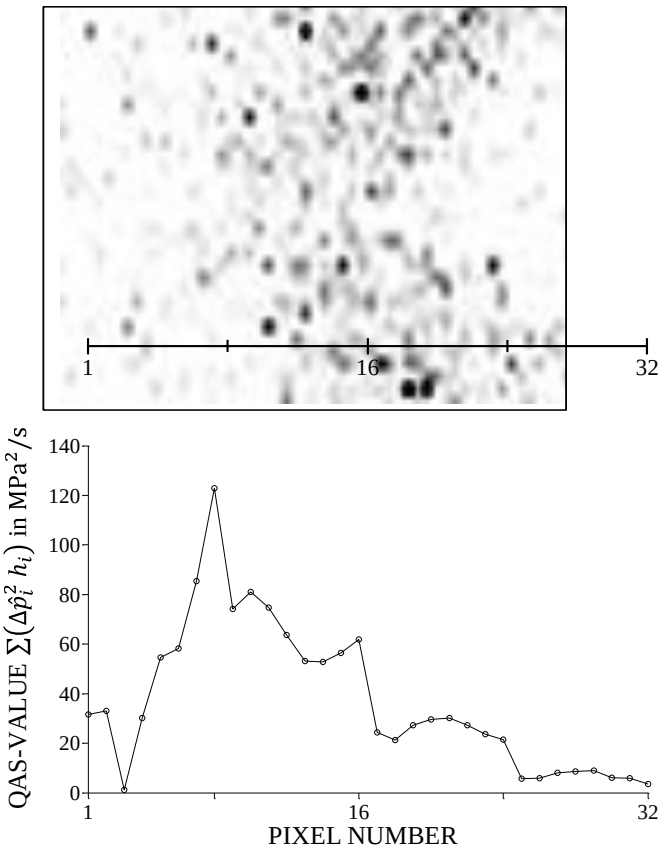

Fig. 6: Comparison of damage map (Pit-Count measurement from [1], upper half of figure) and quadratic amplitude sum determined from measured signals of one pixel line of sensor prototype (lower half of figure) for operating point $\sigma = 5.45$ and $Re = 2.75 \text{ x } 10^5$.

The area of highest cavitation damages determined by the Pit-Count method lies approximately in the range of pixels 10 to 24. In contrast to that, the area of highest quadratic amplitude sum *QAS* and thus intensity of the pressure signals measured with our sensor lies approximately in the range of pixels 5 to 16.

The area of highest expected cavitation damages predicted by the evaluated sensor signals has a slightly smaller width and lies a bit more upstream in comparison with the damage map determined with the Pit-Count method. Both deviations are in agreement with the observations of [1]: For operating conditions with higher cloud cycle frequencies the area of highest cavitation damages is smaller and located more upstream by tendency (we measured collapse frequencies of approximately 43 Hz and [1]

measured detachment frequencies of approximately 38 Hz for the operating condition investigated in the present paper).

One major difference between the two measurement methods is the huge difference in time effort required to perform single measurements. The evaluation of one single operation point by means of the Pit-Count method takes approximately 90 min of exposition of the copper foil to cloud cavitation in order to have well measurable damages, several hours to assemble the nozzle in the test bench and approximately 20 h of evaluation time for the investigation of the copper foil by means of an automated optical measurement system. In contrast to that, as it was shown above, comparable results for single operating points can be acquired (even temporally resolved) with help of the new sensor within seconds.

CONCLUSIONS

Within the present paper a feasibility study for a new cavitation measurement method developed at the *Chair of Fluid Systems Technologies* (TU Darmstadt) was performed. Qualitative comparisons of measurement signals with high-speed photographs were carried out and it was shown that the measurement method is able to measure the pressure signals of cloud cavitation both temporally and spatially resolved.

Further qualitative comparisons of statistically evaluated measurement signals from the new sensor with damage maps acquired by means of Pit-Count measurements were carried out. These proved that the measurement method is able to deliver comparable results concerning the areas of highest cavitation damages with much lower time effort than traditional erosion experiments.

In order to fully combine the advantages of temporal resolved measurements by means of pressure transducers with those of spatially resolved but temporally cumulated measurements by means erosion experiments, the measured area of the sensor respectively its spatial resolution has to be increased without reducing the sampling rate in the future.

OUTLOOK

Considering the measured number of pixels respectively the temporal resolution of our measurement method, we currently work on promising measurement electronics which might enable us to increase the number of recorded pixels to the range of 512 with a sampling rate per pixel in the range of 20 MHz in the near future.

In order to increase the spatial resolution to values above 12 pixels/mm^2 which is the current state of the art in manufacturing of flexible circuit boards, different manufacturing technologies have to be explored during the further development of this promising measurement method.

ACKNOWLEDGMENTS

The authors would like to thank Thomas Keil for his great support in realization of the measurements presented in this paper and for his help with the cavitation phenomena arising in the test bench at the *Chair of Fluid Systems Technologies*.

NOMENCLATURE

b	:	thickness of membrane
$\bar{c}$	:	mean flow velocity
d_{33}	:	piezoelectric distortion coefficient
ε	:	permeability
h_i	:	probability of pressure change class i per time
H	:	channel height
ν	:	kinematic viscosity
p_o	:	outlet pressure
p_v	:	vapour pressure
Δp	:	pressure difference
$\Delta\hat{p}_i$	:	amplitude of pressure change class i
QAS	:	quadratic amplitude sum
Re	:	Reynolds number
ρ	:	density
σ	:	cavitation number
ΔU	:	measurement voltage

REFERENCES

[1] Keil, T., Pelz, P. F., Cordes, U., and Ludwig, G., 2011. "Cloud cavitation and cavitation erosion in convergent divergent nozzle". In WIMRC 3rd International Cavitation Forum 2011, University of Warwick, UK.

[2] Konno, A., Kato, H., Yamaguchi, H., and Maeda, M., 2002. "On the collapsing behavior of cavitation bubble clusters". *JSME International Journal,* ***45***, pp. 631–637.

[3] Pelz, P., and Keil, T., 2012. "Cloud cavitation and cavitation erosion". In *Advanced Experimental and Numerical Techniques for Cavitation Erosion Prediction*. J. P. Chahine, J.P. Franc and K.H. Karimi.

[4] Pelz, P., and Buttenbender, J., 2012. "The influence of imposed strain rate and circulation on bubble and cloud dynamics". In Proceedings of the 8th International Symposium on Cavitation, Singapore.

[5] Reisman, G. E., Wang, Y.-C., and Brennen, C. E., 1998. "Observations of shock waves in cloud cavitation". *Journal of Fluid Mechanics,* ***355***, pp. 255–283.

[6] Schuller, W., 1995. "Akustische Signale und lokale Druckimpulse als Maß für die hydrodynamische Intensität der Kavitation". PhD thesis, TU Darmstadt.